

Magnetic-field effects on photon-induced quantum transport in a single dot-cavity system

Nzar Rauf Abdullah,^{1,2,*} Aziz H. Fatah,¹ and Jabar M. A. Fatah¹

¹*Physics Department, Faculty of Science and Science Education,
School of Science, University of Sulaimani, Kurdistan Region, Iraq*

²*Science Institute, University of Iceland, Dunhaga 3, IS-107 Reykjavik, Iceland*

In this study, we show how a static magnetic field can control photon-induced electron transport through a quantum dot system coupled to a photon cavity. The quantum dot system is connected to two electron reservoirs and exposed to an external perpendicular static magnetic field. The propagation of electrons through the system is thus influenced by the static magnetic and the dynamic photon fields. It is observed that the photon cavity forms photon replica states controlling electron transport in the system. If the photon field has more energy than the cyclotron energy, then the photon field is dominant in the electron transport. Consequently, the electron transport is enhanced due to activation of photon replica states. By contrast, the electron transport is suppressed in the system when the photon energy is smaller than the cyclotron energy.

PACS numbers: 42.50.Pq, 73.23.-b, 78.20.Jq, 75.47.-m

I. INTRODUCTION

Quantum dot (QD) is a crucial electronic structure in the technological devices [1–3] because of its unique properties such as zero-dimensional confinement effect [4] and single electron charge effect (Coulomb blockade) [5]. There are several methods that have been used to control electron motion in QD system. One of which is to control the energy levels and the electron concentration in the QD systems using a plunger gate voltage [6]. On the other hand, by applying a photon radiation that interacts with the electrons in the QD arising a fascinated physical phenomena called photon-assisted tunneling (PAT) [6, 7]. PAT occurs in quantum systems when a photon radiation is applied to an electronic island connected to electron reservoirs [8]. The photon radiation forms extra channels in the electronic island leading to a modification in the electron transport [9]. Therefore, the photon radiation can play an essential role in the transport process generating a photo-current that depends on the photon frequency [10]. Recently, the influences of photon field, in a vacuum state, on two level electronic system [11], and double quantum dots in the presence of a single mode micro-cavity system with both continuous wave and pulsed excitation are studied [12]. Based on the proposed schemes, a single photon generation can be obtained separately under both QD-cavity resonant and off-resonant conditions. The single photon source, in turn, becomes increasingly important in the very diverse range of technological applications.

In addition, external magnetic fields can be used to control the electron transport in nanodevices, which leads to several important effective including the change of the energy level spacing inside the QD [13] and hence the QD lowest energy state shrinks with increasing the magnetic

field. As a result, the Coulomb interaction between two spin degenerate electron grows [14]. Furthermore, external magnetic field can form the edge state [15] and the localized state [16] in the electronic systems, and consequently, the electron transport is reduced.

The combination of the aforementioned fields, namely the magnetic and photon fields, can result in a magneto-photon current in graphene [17] and superconductor [18]. In this work, we have considered magneto-photo transport under the influence of a quantized single photon mode in a cavity and investigated its effect on electron transport through a QD system. In the presence of the photon cavity, extra channels are formed in the system which open new windows for electron tunneling called photon-assisted tunneling process. In addition, we have also shown how an external static magnetic field can control photon-assisted tunneling in the QD system.

This paper is organized as following: In II the description of the model and the theoretical formalism are shown. In III we demonstrate the results. In the last section, IV, conclusions will be presented.

II. MODEL AND THEORY

The system under investigation is a two-dimensional (2D) electron gas exposed to an external static magnetic field and a quantized photon field at low temperature. We assume that the electronic system consists of a quantum dot embedded in a quantum wire. The QD system is connected to two electron reservoirs with different chemical potentials. The electron-photon coupling system is described by the following Hamiltonian in the many-body (MB) basis

$$\hat{H} = \hat{H}_e + \hat{H}_\gamma + \hat{H}_{e-\gamma}, \quad (1)$$

* nzar.r.abdullah@gmail.com

where H_e is the Hamiltonian of the electronic system including electron-electron interaction

$$\hat{H}_e = \int dr \hat{\psi}^\dagger(\mathbf{r}) \left[\frac{\boldsymbol{\pi}^2}{2m^*} + \frac{1}{2}m^*\Omega_0^2 y^2 + U_{\text{Dot}} + eU_{\text{pg}} \right] \hat{\psi}(\mathbf{r}) + \int dr \int dr' \hat{\psi}^\dagger(\mathbf{r}) \hat{\psi}^\dagger(\mathbf{r}') U_C(\mathbf{r}, \mathbf{r}') \hat{\psi}(\mathbf{r}') \hat{\psi}(\mathbf{r}). \quad (2)$$

Herein, $\boldsymbol{\pi} = \mathbf{p} + (e/c)\mathbf{A}$ with \mathbf{p} and $\mathbf{A} = -By\hat{\mathbf{x}}$ being the canonical momentum and magnetic vector potential, respectively. The magnetic field is applied along the z -axis, i.e $\mathbf{B} = B\hat{\mathbf{z}}$, and $\hat{\psi}(\mathbf{r}) = \sum_i \psi_i(r)d_i$ and $\hat{\psi}^\dagger(\mathbf{r}) = \sum_i \psi_i^*(r)d_i^\dagger$ are the fermionic field operators with $d_i(d_i^\dagger)$ being the annihilation(creation) operators for an electron in the single electron state $|i\rangle$ corresponding to ψ_i . The QD potential can be described by

$$U_{\text{Dot}} = Ue^{(-\alpha_x^2 x^2 - \alpha_y^2 y^2)}. \quad (3)$$

Where U is the strength of the potential, and α_x and α_y are constants that determine the diameter of the QD. The plunger-gate voltage is described by U_{pg} which is an electrostatic potential shifting the energy states of the QD system with respect to the chemical potential of the leads. The second term of Eq. (2) indicates the electron-electron interaction in the central system with U_C being the Coulomb interaction potential [19].

The second part of the Eq. (1) can be written as $H_\gamma = \hbar\omega_\gamma a^\dagger a$ introducing the Hamiltonian of the free photon field with $\hbar\omega_\gamma$ being the photon energy and $a(a^\dagger)$ the photon annihilation(creation) operators. The quantized vector potential of the cavity photon field, in the Coulomb gauge, is given by $\hat{\mathbf{A}}_\gamma = A(\hat{a} + \hat{a}^\dagger)\mathbf{e}$ where A is the amplitude of the photon field, related to the electron-photon coupling constant via $g_\gamma = eAa_w\Omega_w/c$, and \mathbf{e} determines the photon polarization with either parallel $\mathbf{e} = \mathbf{e}_x$ or perpendicular $\mathbf{e} = \mathbf{e}_y$ to the electron motion. Note that a_w is the effective magnetic length and Ω_w is the effective confinement frequency of electrons of the QD system.

The last term on the right side of Eq. (1),

$$\hat{H}_{e-\gamma} = -\frac{1}{c} \int dr \mathbf{j}(\mathbf{r}) \cdot \mathbf{A}_\gamma - \frac{e}{2m^*c^2} \int dr \rho(\mathbf{r}) A_\gamma^2, \quad (4)$$

represents the full electron-photon interaction including both para- and dia-magnetic electron-photon interactions, respectively. The charge is $\rho = -e\psi^\dagger\psi$ and the charge current density is governed by

$$\mathbf{j} = -\frac{e}{2m^*} \{ \psi^\dagger (\boldsymbol{\pi}\psi) + (\boldsymbol{\pi}^*\psi^\dagger) \psi \}. \quad (5)$$

The electron-electron and the electron-photon interactions are treated by exact diagonalization in appropriately truncated Fock-spaces.

Figure 1 shows the schematic diagram of the quantum dot system (brown color) connected to two the leads (black color) under the combined effects of the magnetic field B (red arrows) and the photon radiation (blue zigzag

arrows). The chemical potential of the left lead μ_L is assumed to be higher than that of the right lead μ_R . Consequently, the transport is dominated by the left to right electron motions between the two leads through the central system as indicated by pink arrows.

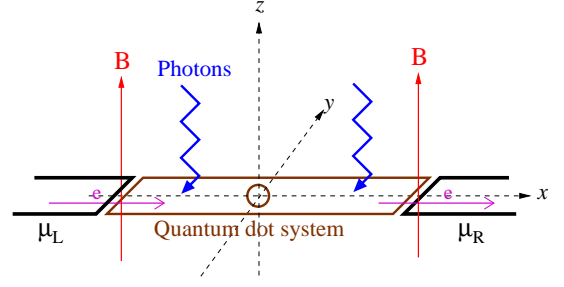


FIG. 1. (Color online) Schematic diagram of a quantum dot system (brown color) connected to the left lead (black color) with chemical potential μ_L and the right lead with chemical potential μ_R . The photon field is represented by the blue zigzag arrows. The external magnetic field B is labeled by a red arrows.

The Liouville-von Neumann equation is used to describe the time-evolution of the many-body density operator of the closed system. But in the case of open system when the central system is connected to the leads, we use a projection operator technique to derive a generalized master equation for the reduced density operator [20, 21]. Since we are interested in the transient behavior of the system, we assume a non-Markovian approach valid to a weak coupling of the leads to the central system [16].

Once we have the reduced density operator, one can calculate charge current and charge density in the system. The charge current is $I^c(t) = I^L(t) - I^R(t)$, where $I^L(t)$ indicates the partial current from the left lead into the QD system and $-I^R(t)$ refers to the partial current into the right lead from the QD system. The partial current can be introduced as $I^{L,R} = \text{Tr}[\dot{\rho}_S^{L,R}(t)\hat{Q}]$ where $\dot{\rho}_S^L$ and $\dot{\rho}_S^R$ are the time derivatives of the system's reduced density matrix due to its coupling to the left and right leads, respectively, [19, 22] and $\hat{Q} = e\hat{N}$ is the charge operator with the number operator \hat{N} .

III. RESULTS AND DISCUSSIONS

We assume the QD system and the leads are made of GaAs semiconductor with effective electron mass $m^* = 0.067m_e$ and relative dielectric constant $\kappa = 12.4$. The parameters of the QD potential are $U = -3.3$ meV, and $\alpha_x = \alpha_y = 0.03$ nm⁻¹. The cavity consists of a single photon mode with energy $\hbar\omega_\gamma = 0.3$ meV, and the electron-photon coupling strength $g_\gamma = 0.1$ meV. The chemical potential of the left and the right leads are $\mu_L = 1.2$ meV and $\mu_R = 1.1$ meV, respectively, implying the bias voltage $\Delta\mu = \mu_L - \mu_R = 0.1$ meV. The temperature of the leads before coupling to the QD sys-

tem is $T = 0.001$ K. The confinement energy of electrons in the QD system is equal to that of the leads $\hbar\Omega_0 = \hbar\Omega_l = 2.0$ meV. Finally, the photon field is linearly polarized and aligned with x -axis parallel to the direction of electron motion in the QD system.

In what follows, we explain the influences of the magnetic field on photon-induced electron transport through the QD system. Figure 2 shows the energy spectrum of the QD system versus the plunger-gate voltage including zero-electron states (0ES, golden diamonds) one-electron states (1ES, blue rectangles) and two-electron states (2ES, red circles). The chemical potential of the leads are indicated by two horizontal lines (black lines).

In Fig. 2(a) the many-electron (ME) energy of the QD system, excluding the photon cavity, is demonstrated. For the selected range of the plunger-gate voltage, the

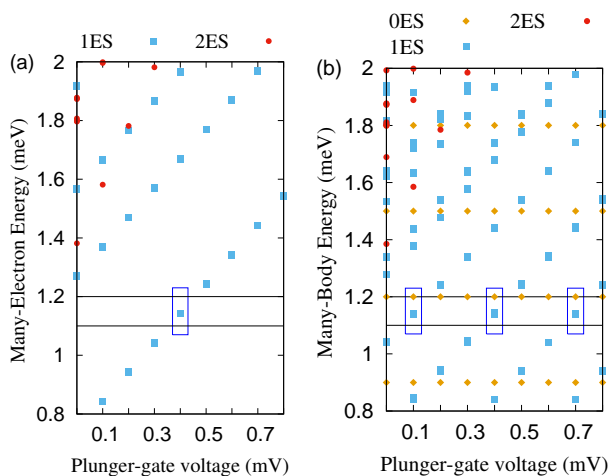


FIG. 2. (Color online) The energy spectrum of the QD system without (a) and with (b) photon cavity versus the plunger-gate voltage U_{pg} including zero-electron states (0ES, golden diamonds), one-electron states (1ES, blue rectangles) and two-electron states (2ES, red dots). The chemical potentials are $\mu_L = 1.2$ meV and $\mu_R = 1.1$ meV (black). The SE state in the bias window is almost doubly degenerate due to the small Zeeman energy.

first excited state lies between the two chemical potential, inside the bias window, which in turn gets into resonance with first subband energy of the leads located in the bias window. Therefore, an electron in the first subband of the left lead may perform electron tunneling into the first-excited state of the QD-system. As a result, a peak in the charge current is formed at $U_{pg}^0 = 0.4$ mV as is shown in Fig. 3. In addition, it should be known that the ground state energy of the QD system is found below 0.8 meV (not shown).

In Fig. 3(a) the charge current versus the plunger-gate voltage U_{pg} is plotted for three different values of the cyclotron energy $\hbar\omega_c \simeq 10^{-4}$ meV (blue solid), 0.34 meV (green dashed) and 0.86 meV (red dotted) corresponding to the magnetic field $B = 0.0001$ T, 0.2 T and 0.5 T,

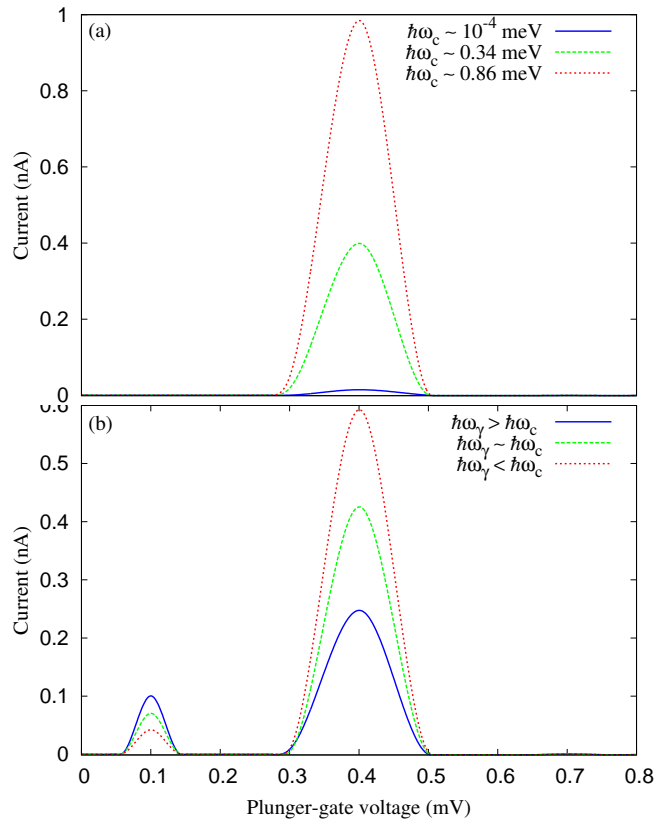


FIG. 3. (Color online) The charge current I_Q is plotted as a function of plunger gate voltage U_{pg} at time $t = 220$ ps for (a) the QD system without photon cavity for cyclotron energy $\hbar\omega_c \simeq 10^{-4}$ meV (blue solid), 0.34 meV (green dashed) and 0.86 meV (red dotted), and (b) the QD system with photon cavity for $\hbar\omega_\gamma > \hbar\omega_c$ (blue solid), $\hbar\omega_\gamma \simeq \hbar\omega_c$ (green dashed) and $\hbar\omega_\gamma < \hbar\omega_c$ (red dotted) where the photon energy is $\hbar\omega_\gamma = 0.3$ meV. The bias window is $\Delta\mu = 0.1$ meV, $g_\gamma = 0.1$ meV, and $N_\gamma = 2$.

respectively. We can clearly see that the peak current is increased with the cyclotron energy. At $\hbar\omega_c \simeq 10^{-4}$ meV the charge current is very weak. This can be attributed to localization of charge density in the QD (see Fig. 4(a)). In contrast, for higher value of cyclotron energy (such as $\hbar\omega_c \simeq 0.86$ meV) corresponding to the higher magnetic field, the charge is delocalized and slightly extended to outside of the QD which can be understood as follows. The high magnetic field induces stronger Lorentz force that forms a circular motion of the electron charge density outside the dot (not shown), and consequently, the charge current is enhanced (see Fig. 3(a) red dotted line).

Now assuming the QD system is coupled to the cavity photon, the electron transport can be affected by both the static magnetic and the dynamic photon fields. For a photon energy $\hbar\omega_\gamma = 0.3$ meV and the electron-photon coupling strength $g_\gamma = 0.1$ meV, Fig. 2(b) demonstrates how the many-body (MB) energy varies as a function of the plunger-gate voltage. In the presence of the cavity,

photon replica states are formed with different photon contents. The energy spacing between the photon replica states is appropriately equal to the photon energy at low electron-photon coupling strength. Therefore, the first-excited state in the bias window is not active anymore in the electron transport, but instead, the electrons from the left leads transfer to the photon replica of the first-excited state in the QD system. Comparing to the energy spectrum of the QD system in Fig. 2(a) for which the photon field is neglected, in Fig. 2(b) two photon replica states at $U_{\text{pg}} = 0.1$ and 0.7 mV (blue rectangles) are found in the bias window corresponding to $U_{\text{pg}} = U_{\text{pg}}^0 - \hbar\omega_\gamma$ and $U_{\text{pg}} = U_{\text{pg}}^0 + \hbar\omega_\gamma$, respectively.

Figure 3(b) shows the charge current as a function of the plunger-gate voltage in the presence of the photon cavity for three cases $\hbar\omega_\gamma > \hbar\omega_c$ (blue solid), $\hbar\omega_\gamma \simeq \hbar\omega_c$ (green dashed) and $\hbar\omega_\gamma < \hbar\omega_c$ (red dotted) where the photon energy is $\hbar\omega_\gamma = 0.3$ meV. The peak current (main-peak) at $U_{\text{pg}}^0 = 0.4$ mV is again found. In addition to the main peak an extra side peak is observed at $U_{\text{pg}} = U_{\text{pg}}^0 - \hbar\omega_\gamma$. The existence of this side peak is due to the formation of the one photon replica of the first excited state.

In the case of $\hbar\omega_\gamma > \hbar\omega_c$, where $\hbar\omega_\gamma = 0.3$ meV and $\hbar\omega_c \simeq 10^{-4}$ meV, the photon field is dominant. Comparing to the charge current in the absence of the cavity shown in Fig. 3(a) (blue solid), the current is increased in the main peak at $U_{\text{pg}}^0 = 0.4$ mV which attributes to the fact that the charge density is stretched out of the QD as is shown in Fig. 4(b). This stretching effect is caused by the paramagnetic term of the electron-photon interaction. In a addition, the contribution of photon replica state with two photons can also lead to the enhances the charge current. It is worth mentioned that this is because the energy of two photon replica state is higher than that of the first-excited state in the energy spectrum. The higher states in the energy spectrum are less bound in the system and actively contribute to the electron transport.

We should also note that the current is almost unchanged when $\hbar\omega_\gamma \simeq \hbar\omega_c$ (green dashed) with $\hbar\omega_c \simeq 0.34$ meV at the main peak recapturing the same value of current as it was found in absence photon cavity.

In addition, when $\hbar\omega_\gamma < \hbar\omega_c$ (Fig. 3(b) red dotted) with $\hbar\omega_c \simeq 0.86$ meV the magnetic field effect is dominant. At this high cyclotron energy the energy spacing between photon replica states are increased and the photon replica states weakly contribute to the electron transport. As a result, the charge current is decreased in the main peak.

Another interesting aspect of this issue is the influence of the external magnetic field on the current in the side peak displayed in Fig. 3(b). The formation of side peak is totally due to the photon cavity. It can be clearly seen that the current is high at low cyclotron energy when $\hbar\omega_\gamma > \hbar\omega_c$ (blue solid) indicating that the photon-induced current should be generated at low magnetic field. There are two reasons for the high

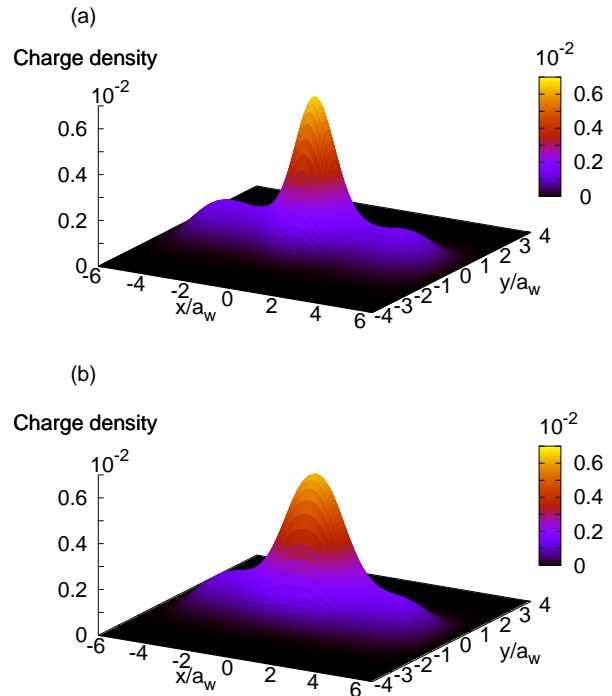


FIG. 4. (Color online) Charge density in the QD system at $t = 220$ ps without (a) with (b) photon cavity in the main current peak at $U_{\text{pg}}^0 = 0.4$ mV shown in Fig. 3 for the cyclotron energy $\hbar\omega_c = 10^{-4}$ meV. The effective magnetic length is $a_w = 33.72$ nm, $\hbar\omega_\gamma = 0.3$ meV, $g_\gamma = 0.1$ meV and $N_\gamma = 2$.

current here: the photon replica states are more active in the electron transport at low cyclotron energy, and the stretching of charge density in the QD system due to the photon cavity. To explain the enhancement of current at the side peak, the charge density at $U_{\text{pg}} = 0.1$ mV is shown in Fig. 5 for (a) the low cyclotron energy ($\hbar\omega_c \simeq 10^{-4}$ meV), i.e. $\hbar\omega_\gamma > \hbar\omega_c$, and (b) the high cyclotron energy ($\hbar\omega_c \simeq 0.86$ meV), i.e. $\hbar\omega_\gamma < \hbar\omega_c$. In Fig. 5(a) the charge density is mostly distributed outside the QD and near the contact area to the leads. The charge accumulation in the contact area leads to the stronger charging to the QD system from the leads, and then the charge current at the side peak is increased. Therefore, we emphasize that the PAT process requires the following condition $\hbar\omega_\gamma > \hbar\omega_c$.

By contrast, at high cyclotron energy ($\hbar\omega_c \simeq 0.86$ meV) when $\hbar\omega_\gamma < \hbar\omega_c$, the magnetic field dominates the electron transport. The magnetic field causes the charge accumulation around the QD as is shown in Fig. 5(b), and then the current is reduced at the side peak.

IV. CONCLUSIONS

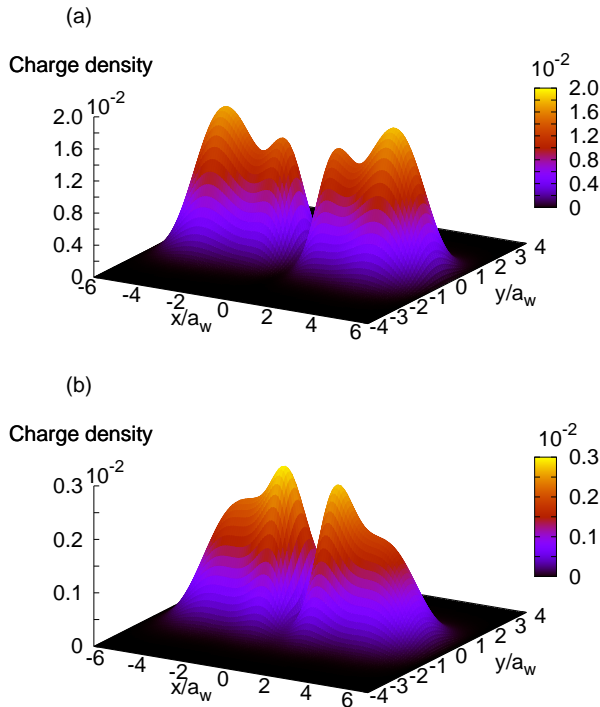


FIG. 5. (Color online) Charge density in the QD system at $t = 220$ ps with photon cavity in the side current peak at $U_{pg} = 0.1$ mV shown in Fig. 3(b) for case of $\hbar\omega_\gamma > \hbar\omega_c$ (a) and $\hbar\omega_\gamma < \hbar\omega_c$ (b). The effective magnetic length is $a_w = 33.72$ nm, $\hbar\omega_\gamma = 0.3$ meV, $g_\gamma = 0.1$ meV and $N_\gamma = 2$.

We have investigated the influences of a static magnetic field on photon-induced transport through a quantum dot coupled to a quantized photon cavity. It was found that the cavity forms photon replica states and their contribution to the electron transport can be affected by the external magnetic field. Therefore, two different regimes are studied, low and high magnetic fields. At the low magnetic field regime (low cyclotron energy) where the cyclotron energy is assumed to be lower than the photon energy, the photon replica states formed in the presence of the cavity are actively contribute to the transport. Consequently, the charge density in the system are stretched and then the current is increased.

On the other hand, at the high magnetic field regime (high cyclotron energy), when the cyclotron energy is higher than the photon energy, the magnetic field is dominant and the photon-induced current is suppressed. As a result, we emphasize that the photon-induced transport or photon-assisted transport can be obtained when the the photon energy is higher than the cyclotron energy in the system.

ACKNOWLEDGMENTS

Financial support is acknowledged from the Icelandic Research and Instruments Funds, and the Research Fund of the University of Iceland. The calculations were carried out on the Nordic High Performance Computer Center in Iceland. We are thankful to Dr. Peshwaz Abdoul for very interesting discussions. We acknowledge the Nordic network NANOCONTROL, and The University of Sulaimani.

-
- [1] A. Imamoglu and Y. Yamamoto. Turnstile device for heralded single photons: Coulomb blockade of electron and hole tunneling in quantum confined $p-i-n$ heterojunctions. *Phys. Rev. Lett.*, 72:210–213, Jan 1994.
 - [2] D. Loss and D. P. DiVincenzo. Quantum computation with quantum dots. *Physical Review A*, 57(1):120, 1998.
 - [3] D. P. DiVincenzo. Double quantum dot as a quantum bit. *Science*, 309, 2173 2005.
 - [4] Pierre M. Petroff, Klaus H. Schmidt, Gilberto Medeiros Ribeiro, Axel Lorke, and Jorg Kotthaus. Size Quantization and Zero Dimensional Effects in Self Assembled Semiconductor Quantum Dots. *Japanese Journal of Applied Physics*, 36(6S):4068, 1997.
 - [5] LeoP. Kouwenhoven and PaulL. McEuen. Single Electron Transport Through a Quantum Dot. In Gregory Timp, editor, *Nanotechnology*, pages 471–535. Springer New York.
 - [6] T. Fujisawa, W. G. van der Wiel, and L. P. Kouwenhoven. Inelastic tunneling in a double quantum dot coupled to a bosonic environment. *Physica E*, 7:413–419, 2000.
 - [7] L. P. Kouwenhoven, S. Jauhar, K. McCormick, D. Dixon, P. L. McEuen, Yu. V. Nazarov, N. C. van der Vaart, and C. T. Foxon. Photon-assisted tunneling through a quantum dot. *Phys. Rev. B*, 50:2019–2022, Jul 1994.
 - [8] K. Shibata, A. Umeno, K. M. Cha, and K. Hirakawa. Photon-Assisted Tunneling through Self-Assembled InAs Quantum Dots in the Terahertz Frequency Range. *Phys. Rev. Lett.*, 109:077401, Aug 2012.
 - [9] K Ishibashi and Y Aoyagi. Interaction of electromagnetic wave with quantum dots. *Physica B*, 314:437–443, 2002.
 - [10] L. P. Kouwenhoven, S. Jauhar, J. Orenstein, P. L. McEuen, Y. Nagamune, J. Motohisa, and H. Sakaki. Observation of Photon-Assisted Tunneling through a Quantum Dot. *Phys. Rev. Lett.*, 73:3443–3446, Dec 1994.
 - [11] Nie Wen-Jie Guo Yu-Jie. *Chinese Physics B*, 24(9):94205, 2015.
 - [12] Yu Zhong-Yuan Zhang Wen Liu Yu-Min Ye Han, Peng Yi-Wei. Sub-Poissonian photon emission in coupled double quantum dots–cavity system. *Chinese Physics B*, 24(11):114202, 2015.
 - [13] P. A. Maksym and Tapash Chakraborty. Quantum dots in a magnetic field: Role of electron-electron interactions. *Phys. Rev. Lett.*, 65:108–111, Jul 1990.
 - [14] W. G. van der Wiel, S. De Franceschi, J. M. Elzerman, T. Fujisawa, S. Tarucha, and L. P. Kouwenhoven. Electron transport through double quantum dots. *Rev. Mod.*

- Phys.*, 75:1–22, Dec 2002.
- [15] Thomas Ihn. *Semiconductor Nanostructures*. Oxford University Press, New York, US, 2010.
- [16] Nzar Rauf Abdullah, Chi-Shung Tang, and Vidar Gudmundsson. Time-dependent magnetotransport in an interacting double quantum wire with window coupling. *Phys. Rev. B*, 82:195325, Nov 2010.
- [17] David Hagenmüller and Cristiano Ciuti. Cavity QED of the Graphene Cyclotron Transition. *Phys. Rev. Lett.*, 109:267403, Dec 2012.
- [18] Curdin Maissen, Giacomo Scalari, Federico Valmorra, Mattias Beck, Jérôme Faist, Sara Cibella, Roberto Leoni, Christian Reichl, Christophe Charpentier, and Werner Wegscheider. Ultrastrong coupling in the near field of complementary split-ring resonators. *Phys. Rev. B*, 90:205309, Nov 2014.
- [19] N. R. Abdullah. *Cavity-photon controlled electron transport through quantum dots and waveguide systems*. PhD Thesis, University of Iceland, Reykjavik, Iceland (2015).
- [20] S. Nakajima. On quantum theory of transport phenomena steady diffusion. *Prog. of Theor. Phys.*, 20:948, 1958.
- [21] Robert Zwanzig. Ensemble Method in the Theory of Irreversibility. *The Journal of Chemical Physics*, 33(5):1338–1341, 1960.
- [22] Nzar Rauf Abdullah, Chi-Shung Tang, Andrei Manolescu, and Vidar Gudmundsson. *ACS Photonics*, 3(2):249–254, 2016.